# **International Journal of Technology**

http://ijtech.eng.ui.ac.id



Research Article

# An Efficient Technique to Remove Acid Gases from Natural Gas with a Hollow Fiber-Based Membrane-Assisted Gas Absorption Unit

Anton N. Petukhov <sup>1,2,\*</sup>, Artem A. Atlaskin <sup>1</sup>, Kirill A. Smorodin <sup>1,2</sup>, Maria E. Atlaskina<sup>1,2</sup>, Dmitriy M. Zarubin <sup>1,2</sup>, Sergey S. Kryuchkov <sup>1</sup>, Anna N. Stepakova <sup>1</sup>, Andrey V. Vorotyntsev <sup>2</sup>, Olga V. Kazarina <sup>1,2</sup>, Sergey S. Suvorov <sup>2</sup>, Ekaterina A. Stepanova <sup>2</sup>, Ilya V. Vorotyntsev <sup>1</sup>

<sup>1</sup>Mendeleev University of Chemical Technology of Russia, Miusskaya square, 9, Moscow 125047 Russia <sup>2</sup>Lobachevsky State University of Nizhny Novgorod, 23 Gagarin Avenue, Nizhny Novgorod, 603950, Russia \*Corresponding author: antonpetukhov@unn.ru, Tel.: +7 (920) 019-49-23

**Abstract:** This paper discusses the development and optimization of a novel technique, membraneassisted gas absorption (MAGA), and its application in the removal of acid gases from natural gas, also known as the natural gas sweetening process. Membrane-assisted gas absorption is a hybrid separation technique that involves the selective absorption of acid gases with further permeance through the membrane. It is a pressure-drive heat-free method that occurs continuously in a steadystate mode. The application of a new gas separation cell design based on different hollow-fiber membranes (polysulfone gas separation and ultrafiltration) is discussed. This allows the ratio between the amount of absorbent and the area of the membrane in contact with it to be decreased. The applied membranes and the cell were characterized using the mass-spectrometry method to obtain the mass transfer properties with respect to the mixed gas. The absorbents were also studied, and their absorption capacity and viscosity were obtained. Based on these experimental data, the design of the optimal membrane-absorbent system was determined. Furthermore, the separation efficiency of the membrane-assisted gas absorption technique was investigated on model (methane, carbon dioxide, and xenon in the ratio of 94.5/5.35/0.15 vol.%) and quasi-real (methane, ethane, carbon dioxide, propane, nitrogen, butane, hydrogen sulfide, and xenon in the ratio: 75.677/7.41/5.396/4.534/3.013/2.469/1.389/0.113 vol.%) gas mixtures. The MAGA unit with 30 wt.% MDEA aqueous solution showed high gas separation efficiency for both mixtures. The MAGA unit can remove up to 96% of sour gases from the mixture. The hydrocarbon losses do not exceed 1%, even in the maximum productivity mode. The overall efficiency of the process can be improved using specific absorbents with aqueous solutions of amino alcohols.

**Keywords:** Gas separation; Hollow fibers; Membrane-assisted gas absorption; Natural gas processing; Sweetening

The main part of the study was supported by the Russian Science Foundation (project no. 22-79-10222). The analytical support was funded by The Ministry of Science and Higher Education of the Russian Federation within the framework of the scientific project of the laboratory «Laboratory of Electronic Grade Substances Technologies», project No. FSSM2022-0005. Mass-transfer properties of the combined membrane-absorbent systems were study was funded by Ministry of Science and Education of the Russian Federation within the framework of the scientific project No. FSSM-2023-0004.

#### 1. Introduction

Civilization development is directly linked to the process of energy generation. In view of the increasingly severe environmental situation, technologies related to waste-free or low-waste methods of energy production play an important role (Liang et al., 2022; Si et al., 2022; Zou et al., 2021; Ostergaard et al., 2020). Natural gas is one of the most environmentally friendly energy sources (Bello and Solarin, 2022; Shirazi et al., 2022; Litvinenko, 2020). Natural gas deposits, both due to geological and other factors (e.g., the biota that became the origin of the deposit), always contain acid gases (CO<sub>2</sub> and H<sub>2</sub>S), so it is necessary to separate acid gases from natural gas. Acid gases reduce fuel's calorific value and create environmental and technological hazards (Rahmani et al., 2023; Khan et al., 2021; Tikadar et al., 2021a; 2021b).

Removal of acid gases is an important step in the preparation of natural gas for transportation and processing (Darani et al., 2021; Liu et al., 2020). Amino-alcohol chemisorption is currently the most common method of purifying natural gas from polluting components (Berchiche et al., 2023; Ellaf et al., 2023; Ibrahim et al., 2022). This method has been actively used and developed for several decades. However, it has some inherent disadvantages (Godin et al., 2021; Davarpanah et al., 2020; Struk et al., 2020). Among the main disadvantages are high capital and operating costs, problematic regeneration of sorbents, low reliability of apparatuses, relatively high complexity of operation and maintenance, large footprint, the necessity of preliminary deep purification of gas, and significant environmental damage from the operation process (Rochelle, 2024; Liu et al., 2021a; Ghasem, 2020). Additionally, amine purification plants are economically efficient only for massive production facilities.

Membrane gas separation is an attractive alternative to amine treatment. The important disadvantages of amine scrubbing are not present (Makertihartha et al., 2022; Liu et al., 2021b; 2021c; Lei et al., 2020; Yahaya et al., 2020; Vorotyntsev et al., 2009; 2006b). Thus, the membrane gas separation method is a reagent- and heat-free technology, where acid gas removal can be performed at ambient temperature using relatively inexpensive polymeric materials (Hazarika and Ingole, 2024; Jana and Modi, 2024; Kryuchkov et al., 2024; Valappil et al., 2021) The interdependence of selectivity and process performance is an important limiting factor in the development of the membrane method. In other words, the more efficient the separation, the lower the rate of this process (Robeson, 2008). Two main approaches to improve membrane separation methods can be distinguished (Khan et al., 2024; Vorotyntsev et al., 2006a). Firstly, new membrane materials can be sought (Bashir et al., 2024; Niu et al., 2024; Singh et al., 2024; Otvagina et al., 2019). However, the interdependence of performance and selectivity still acts as a limiting factor for this approach. Second, new engineering solutions can be sought (Kartohardjono et al., 2023; Karamah et al., 2021).

The group of authors proposed a new method, membrane-assisted gas absorption (MAGA), which is a pressure-controlled hybrid process. In its framework, the separation is continuous; gases are absorbed by a liquid absorbent spread over a membrane. The gases permeate through the membrane after absorption by the liquid. The separation of gas mixtures occurs in a single stage without phase transitions and without the need to maintain high temperatures. Compared to conventional membrane gas separation, the use of a liquid absorbent increases the system's selectivity. An important and significant feature of the method is the self-regeneration of the absorbent, which occurs naturally in the process of gas sorption-desorption cycle and its penetration into the submembrane space. Taking into account the aforementioned, the most significant influence on the process is the choice of membrane and liquid absorbent materials. This imposes some limitations on the possibility of their selection. Thus, the mass transfer rate must be considered. This is because many polymeric materials, being able to effectively separate gas mixtures, cannot provide the required process rate.

A group of authors initially proposed the MAGA method for the removal of acid gases and for ammonia recovery and purification, and the apparatus was based on planar-framed membrane modules (Atlaskin et al., 2021; Kryuchkov et al., 2021; Petukhov et al., 2021). Then, various

improvements of this method were proposed, such as the application of hollow fiber membranes to solve the same problem and the use of ILs as a sorbent in the system (Petukhov et al., 2022; Atlaskin et al., 2020). This study investigates the feasibility of applying the MAGA method to the separation of natural gas flow from sour gases. Modules based on hollow fibers made of PSF and PEI+PI are applied and investigated in this study.

The present work deals with a comprehensive study of materials and processes during natural gas separation using a novel hybrid technique, membrane-assisted gas absorption. During the complex investigation, a combined system comprising absorbent, gas separation, and ultrafiltration membranes was proposed and characterized with respect to its mass transfer properties. The proposed system was implemented during the separation process. The membrane-assisted gas absorption technique may be considered an attractive alternative to conventional methods.

#### 2. Materials and Methods

#### 2.1. Materials

In correspondence to the aim of the present study, special gas mixtures in stainless steel cylinders were prepared to evaluate the membrane-assisted gas absorption technique for natural gas processing, namely, removal of acid gas impurities. The first mixture, designed for the preliminary study, contains three components: methane, carbon dioxide, and xenon in a ratio of 94.5/5.35/0.15 vol.% under a pressure of 4 MPa. The second mixture, identical in composition to natural gas, as mentioned in Patent (Smetannikov et al., 2010) contains eight components: methane, ethane, carbon dioxide, propane, nitrogen, butane, hydrogen sulfide, and xenon in the ratio: 75.677/7.41/5.396/4.534/3.013/2.469/1.389/0.113 vol.% under the same pressure value. The gas mixtures were prepared using pure gases: nitrogen ( $\geq 99.999$  vol.%), methane ( $\geq 99.99$  vol.%), xenon ( $\geq 99.999$  vol.%), ethane ( $\geq 99.94$  vol. %), propane ( $\geq 99.98$  vol.%), butane ( $\geq 99.97$  vol.%), carbon dioxide ( $\geq 99.99$  vol.%), and hydrogen sulfide ( $\geq 99.5$  vol.%) supplied by «NII KM» Ltd, «Vössen M I Y» Ltd, and «Firma Horst» Ltd (Moscow, Russia).

A 30 wt.% aqueous solution of amino alcohol - methyldiethanolamine (MDEA) was used as a liquid absorbent in the process of acid gas capture using a membrane-assisted gas absorption unit. «Oka-Sintez» Ltd (Dzerzhinsk, Russia) provided the methyldiethanolamine. Deionized water obtained using Millipore Direct-Q3 was used to prepare the solutions. Reagents were used without additional purification. Solutions were prepared using the standard gravimetric method on an analytical balance (Shimadzu AUW-220D).

In this study, hollow fiber membranes of polysulfone (PSF) were purchased from Hangzhou Kelin Aier Qiyuan Equipment Co., Ltd. (Hangzhou, China), polyetherimide/polyimide blend (PEI +PI) hollow fibers were provided by the Institute of Macromolecular Chemistry CAS (Prague, Czech Republic) in cooperation with MemBrain s.r.o. company. The studied membranes are based on polysulfone and a polymer blend of polyetherimide (ULTEM 1000) and polyimide (Matrimid 5218), which are hollow fibers with an anisotropic structure and an internal selective layer.

#### 2.2. Methods

A schematic of the experimental setup is shown in Figure 1 illustrates the membrane-assisted gas absorption unit, where the counter-current flow mode is used for the separation process. A schematic of the separation cell, its detailed description, technical data, flat and 3D schemes, and photos are provided in the Supplementary Materials (Figs. S1–S2, Table S1). The source and product flows, namely, feed and retentate, are controlled by mass flow controllers (Bronkhorst, El-Flow Prestige FG-201CV) and pressure transmitters (Wika, S-20). The back pressure regulator (Bronkhorst, EL-Press P-702CM) maintains a constant pressure level in the cell and product line. The pressure on the permeate side is a process-controlled value and is formed by the resistance in the fibers and the flow of permeate gas. In other words, the operator does not manually influence the pressure value. The cell outlets, which are permeate and retentate lines, are connected to a four-port two-position switching valve (VICI, A4VL4MWE2) equipped with a high-speed switching

accessory that allows 8 ms switch performance. It is used to alternately switch analyte flows using a gas chromatography system. The HSSA does not create pneumatic resistance in the line, which is typical for conventional valves, where the switching time exceeds 180 ms. The flow is fed into an analytical system represented by a Chromos GC-1000 gas chromatograph. The sample is separated in the chromatographic column under isothermal conditions, and the signal change is recorded using a thermal conductivity detector. Detailed conditions for GC analysis are presented in Table 1.

**Table 1** Process parameters for gas chromatography analysis

GC Component	Description
Detector	TCD-1, 3 V, 170℃
	TCD-2, 3 V, 170°C
Analytical	Hayesep R 3m×2mm, SS316 stainless steel (SS316), 80/100 mesh
Column	Hayesep Q 3m×2mm, SS316 stainless steel (SS316), 80/100 mesh
	40°C (5.8 min) heat 25°C/min (0.8 min); 60°C (3.6 min) heat 25°C/min (0.8 min); 80°C (2.5
	min) heat 35°C/min (1.57 min); 135°C (9.9 min); 200°C
Sampling loop	1 cm3, 145°C
Carrier gas	He 99.995 vol.%, 20 cm3 min-1

The experiment entails introducing the gas system into the inlet port of the experimental unit via a Drastar pressure regulator to maintain a desired pressure level prior to the mass flow controller, which guarantees an accurate gas flow rate of the separated gas mix. The feed stream enters the MAGA unit, where a combined membrane-absorption system captures acid gas impurities and transfers them to the permeate side. Next, the separated components are captured with carrier gas fed through a pressure regulator and mass flow controller and exit the unit for further analysis. The same process is performed for the retentate, which is depleted of permeated components. The back pressure regulator mounted on the retentate line provides a consistent pressure level throughout the length of the line from its feed to the regulator, ensuring a uniform pressure ratio across the combined system. The permeate and retentate streams were sequentially analyzed via a gas chromatograph to assess the progress of achieving a steady state and the efficiency of the separation process. Table 2 shows the experimental conditions.

**Table 2** Experimental conditions during the membrane-assisted gas absorption process

<u>- I -                                 </u>					
Parameter	Value				
Feed-stream pressure	0.4 MPa				
Permeate pressure	0.104–0.105 MPa				
Feed flow rate	100-150 cm3 min-1				
Temperature	25°C				
Stage-cut	0.05–0.065				

After performing the permeation tests for hollow fibers, the membrane-assisted gas absorption cell was studied. The mass transfer properties of the cell were determined using the method described in the supplementary materials. As the permeate side of the cell is flow-through volume, the helium sweep inlet was stubbed to perform vacuum mode measurements.

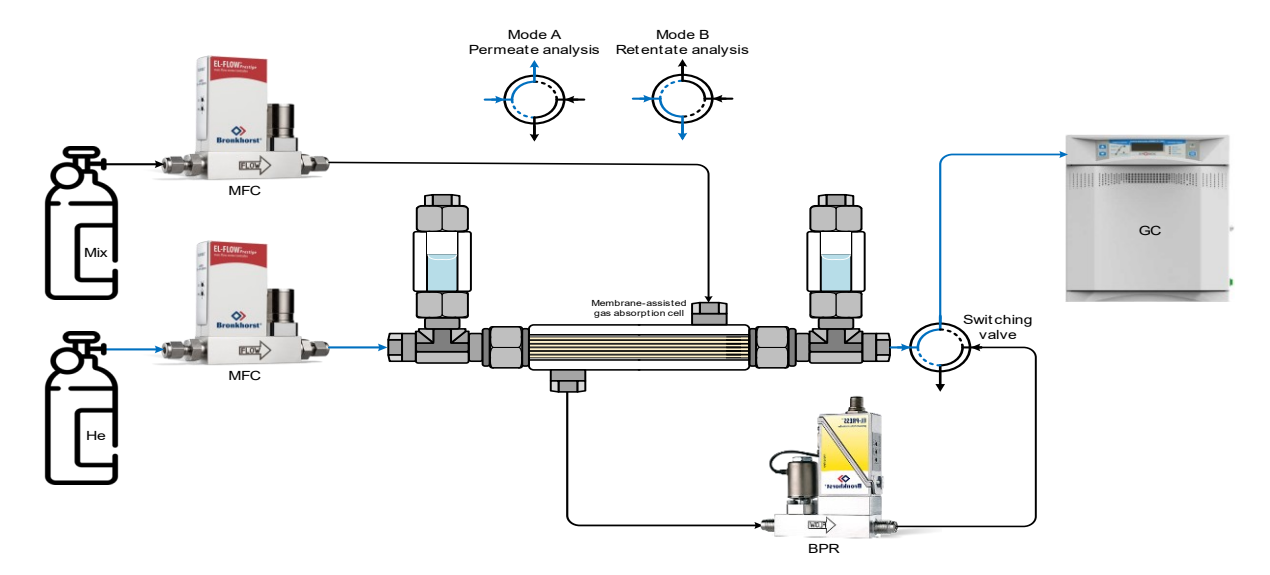


**Figure 1** Principal scheme of the experimental setup for evaluating the separation process using the MAGA technique

### 3. Results and Discussion

# 3.1. Preliminary tests of the absorbent solution

In this study, aqueous solutions of methyldiethanolamine were investigated as absorbents. A special feature of MDEA is that it can be partially regenerated in an instant. As a result, large amounts of acid gases can be removed with a small amount of heat for regeneration (desorption temperature 373 K) (Jamal et al., 2006). Because MDEA is a tertiary amine, it has a lower affinity for H<sub>2</sub>S and CO<sub>2</sub> than DEA. MDEA has several distinct advantages over primary and secondary amines. In addition, the higher resistance to decomposition is characteristical for MDEA. The slowness of the reaction leading to the formation of bicarbonate is the main reason why tertiary amines can be considered as selective for the removal of H<sub>2</sub>S, in cases where the complete removal of CO<sub>2</sub> is not required. Table 3 presents the chemical properties of MDEA.

**Table 3** Chemical properties of the MDEA

Amines	CAS number	Chemical structure	MW(g/mol)
N-methyldiethanolamine (MDEA)	105–59-9		119.16
		но У ОН	

The mechanism of acid gas sorption by amino alcohols is illustrated by the reaction of primary amines with  $CO_2$  and  $H_2S$  (formulas 1-5).

$$2RNH_2 + CO_2 = RNH_3 + RNHCOO$$
 (1)

$$RNH_2 + CO_2 + H2O = RNH_3^+ + HCO_3^-$$
 (2)

$$RNH_2 + HCO_3^- = RNH_3 + + CO_3^{2-}$$
(3)

$$RNH_2 + H_2S = RNH_3^+ + HS^-$$
 (4)

$$RNH_2 + HS = RNH_3^+ + S^2$$
 (5)

The dominant general reaction (Equation 1) with primary and secondary amines quickly leads to the formation of a stable carbamate, which is slowly hydrolyzed to bicarbonate. The other general reactions leading to the formation of bicarbonate (Equation 2) and carbonate (Equation 3) are slow because they must go through the hydration of CO<sub>2</sub>.

Unlike primary and secondary amines, the nitrogen in tertiary amines does not have free hydrogen for the rapid formation of carbamate according to the general equation (1). Consequently, CO<sub>2</sub> removal by tertiary amines can only occur via the slow pathway to bicarbonate according to

equation (2) and carbonate according to equation (3). The main reason why tertiary amines can be considered selective for  $H_2S$  removal when complete  $CO_2$  removal is not required is the slowness of the reaction leading to bicarbonate formation. However, at high partial pressures, the solubility of  $CO_2$  in tertiary amines is much higher than in primary and secondary amines.

As a part of the complex study, preliminary tests of the absorbent systems were performed. To choose the most suitable absorbent, a wide range of MDEA concentrations in aqueous solution were considered and compared with literature data. A comparison was performed to verify the applied experimental technique and evaluate the absorbent properties under conditions that are close to the conditions of the separation process. In accordance with this aim, the MDEA mass fraction was changed from 10 to 40 wt.% with a step of 10 wt.%, while the literature data is given for the 0–60 wt.%.

The application of MDEA is justified by several factors. MDEA does not cause corrosion, is characterized by low saturated vapor pressure, and has a low specific heat capacity and heat of reaction with H<sub>2</sub>S and CO<sub>2</sub>. In 1987, it was possible to reduce the carbon dioxide content in commercial gas to 1–1.4% as a result of processing the natural gas at the Orenburg and Karachaganak oil and gas condensate fields (Nasteka, 1996) using an aqueous solution of MDEA, with an amino alcohol mass content of 30%.

Moreover, based on the data available in the literature, 30% aqueous solutions of MDEA offer the highest absorption capacity among alkanolamines, such as monoethanolamine (MEA) and triethanolamine (TEA). Table 4 shows the absorption capacities of 30% aqueous solutions of MEA, TEA, and MDEA with respect to carbon dioxide.

<b>Table 4</b> Absorption	n capacity o	f various alka	anolamine towa	ard to carbon dioxide
---------------------------	--------------	----------------	----------------	-----------------------

	Absorption	capacity		Reference	
Alkanolamine _	$mol_{CO_2} \cdot mol_{amine}^{-1}$	$mol_{CO_2} \cdot kg_{abs}^{-1}$	_ P, kPa		
	0.59	2.90	100	(Hadri et al., 2015; Yamada et al., 2012)	
MEA	0.60-0.62	2.95-3.05	100	(Mahi et al., 2019; Jou et al., 1995; Dawodu and Meisen, 1994)	
MDEA	0.68	1.71	100	(Fu et al., 2016a; Hadri et al., 2015)	
TEA	0.38	0.76	100	(Rayer et al., 2012)	

The viscosity was measured using an Anton Paar MCR702e rheometer equipped with a PR170/Ti/XL measuring cell, a C-ETD 200/XL/PR temperature sensor, and a PA-23S pressure sensor. MDEA solutions with a mass concentration of 10–40 wt.% were prepared. Measurements were performed at pressures of 100 and 400 kPa for neat and acid gas-rich absorbents, respectively. The PR170/Ti/XL is a measuring cell made of titanium that allows measurements to be performed at elevated pressure values. In that case, the viscosity of the loaded MDEA aqueous solutions was measured in the environment of an eight-component gas mixture.

Moreover, the present study deals with the evaluation of MDEA aqueous solutions CO<sub>2</sub> absorption capacity with different MDEA mass concentrations (similar to described above). The absorption capacity of the solutions was calculated based on the raw data obtained using the gravimetric technique. The weight gain was measured using an analytical balance (VIBRA AF-225DRCE) (Accuracy: 1·10-4/1·10-5 g). Aqueous solutions were loaded into a thin-walled stainless steel cuvette with gas inlet and outlet connectors. The outlet tube is connected to a back pressure regulator (Bronkhorst P702CM), which maintains constant pressure during the experiment. The solubility limit is reached after the weight of the sample stops to change, and the total weight gain is the absorption capacity of the sample. The cell was placed in a thermostat and maintained at

298.15 K. The experiment was conducted at atmospheric pressure (~ 100 kPa) and at an elevated pressure of 400 kPa. The obtained results at atmospheric pressure were compared to literature data, and the absorption capacity at 400 kPa was investigated after the technique was verified. Figure 2 shows the experimental scheme for absorption capacity measurements.

Figure 3 (a, b) shows the results of the preliminary study of absorbents, where the viscosity ( $\eta$ ) and absorption capacity ( $n_{CO_2} \cdot m_{abs}^{-1}$ ) plotted against the MDEA mass fraction in aqueous solutions.

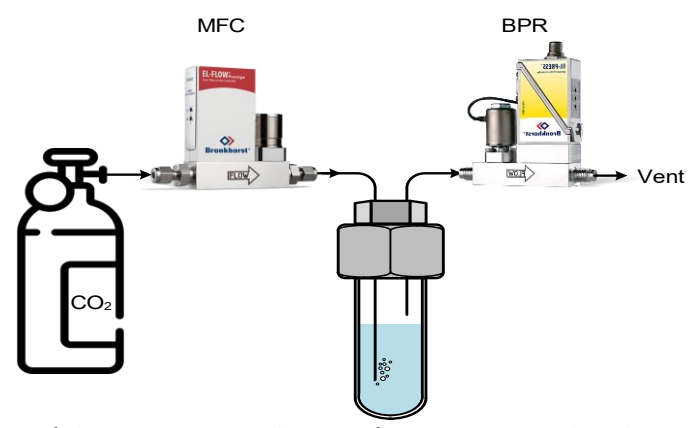
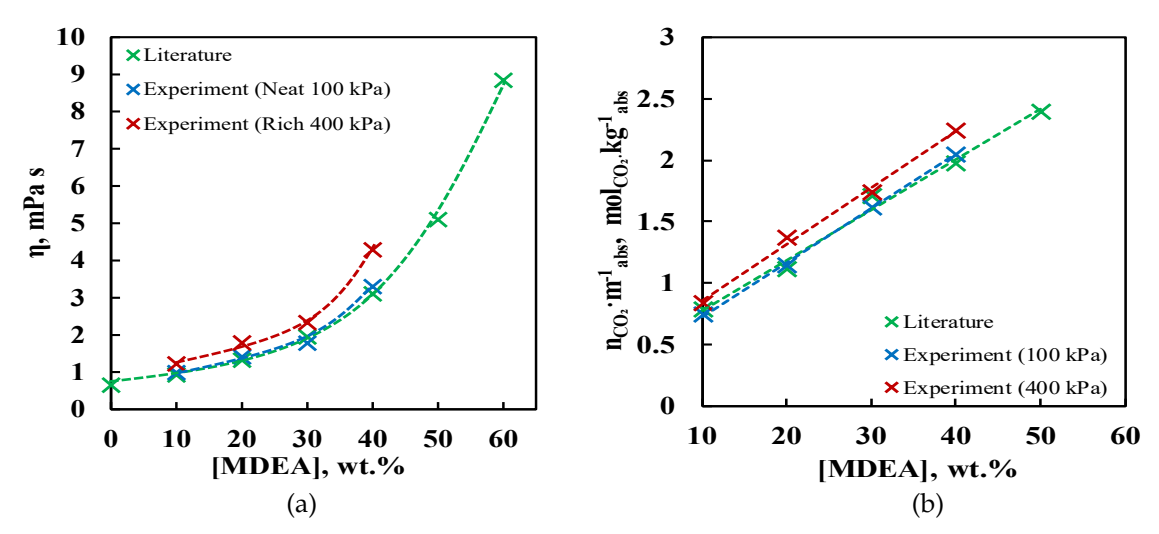


Figure 2 Principal scheme of the experimental setup for measuring the absorption capacity

As shown in Figure 3 (a), the experimentally obtained viscosity values of MDEA aqueous solutions under 100 kPa are close to the data reported in the literature (Fu et al., 2016b; Hadri et al., 2015). Thus, a deviation of no more than 9 % is observed, and based on these results, it may be concluded that the applied technique provides correct measurements. Furthermore, the measuring cell was fed with an eight-component mixture under a pressure of 400 kPa and was maintained for 72 h to ensure that the solution limit was reached. Then, the viscosity measurement was performed. The viscosity of rich MDEA aqueous solutions is higher than the values obtained for neat samples in the entire observed range of solution composition. Thus, for 10 wt.% MDEA content, it is 1.23, for 20 wt.% - 1.79, for 30 wt.% - 2.33, and for 40 wt.% it is 4.29 mPa s. According to the dependence of viscosity on MDEA content, it is of interest to apply the solution from the linear region of viscosity gain – 10–30 wt.%. Increasing the MDEA content from 10 to 20 wt.% increases the viscosity value by 45.9 %, and further increases the MDEA content to 30 wt.%, accompanied by a viscosity gain of up to 84 %.



**Figure 3** (a) Viscosity and (b) absorption capacity of MDEA aqueous solutions with different MDEA mass fractions. The green crosses are data from the literature (Fu et al., 2016b; Hadri et al., 2015); the blue crosses are experimental data obtained in the present study as a verification of techniques;

the red crosses are experimental data for loaded MDEA aqueous solutions under elevated pressure (left) and data obtained at elevated pressure during CO<sub>2</sub> absorption (right)

Thus, the higher viscosity of CO<sub>2</sub> loaded solutions is observed due to the increase in intermolecular forces between aqueous amine molecules, CO<sub>2</sub>, and reaction products.

Figure 3 (b) illustrates the influence of MDEA content on the absorption capacity of different MDEA aqueous solutions. As shown in the graphs, all considered cases are linear. The figure shows three curves: literature data; experimental data obtained under the same conditions; and experimental data obtained at an elevated pressure of 400 kPa. The experimentally found absorption capacity values at 100 kPa agree well with the literature data. This allows us to conclude that the applied technique is appropriate and provides correct data. The same tests were performed at the pressure of 400 kPa pure CO<sub>2</sub>. It was found that the absorption capacity dependence is also linear and overcomes the values obtained at 100 kPa. The absorption capacity gain was up to 23.4 % compared with the literature data and values obtained at 100 kPa of CO<sub>2</sub>. Considering the linear growth of the MDEA aqueous solutions CO<sub>2</sub> absorption capacity observed for all considered compositions, the criterion of suitability is the viscosity value, as it influences the mass transfer characteristics, namely the diffusion component.

According to the Stokes-Einstein-Sutherland equation, the diffusion coefficients of gas into the liquid absorbent system can be evaluated:

$$D = \frac{k_B T}{6\pi \eta t'} \tag{4}$$

where D is the diffusivity coefficient of gas A in liquid B, cm<sup>2</sup> s<sup>-1</sup>;  $k_B$  is the Boltzmann constant; T is the temperature, K;  $\eta$  – dynamic viscosity, mPa s; and r is the particle radius, m. The Stokes-Einstein-Sutherland relation was used to calculate the diffusion coefficients. For technological calculations, a factor of 4  $\pi$  rather than 6  $\pi$  is often used. It is important to note that the values predicted by this equation are only estimates.

Figure 4 shows the results of the diffusion coefficients estimation. The maximum values of CO<sub>2</sub>, H<sub>2</sub>S, and CH<sub>4</sub> diffusion coefficients are observed at 10 wt.% MDEA content. Increasing the MDEA concentration to 30 wt.% decreased the diffusion coefficients almost twice (1.9 times) compared with the 10 wt.% MDEA aqueous solution. Meanwhile, at 40 wt.% MDEA, the diffusion coefficients were 3.5 times lower. The absorption capacity of 30 wt.% MDEA content is 2.1 times higher than that of 10 wt.% MDEA aqueous solution. Increasing the MDEA content up to 40 wt.% increases the absorption capacity by 2.7 times. Considering the complex of the obtained results, it may be concluded that the optimal absorbing solution composition is a 30 wt.% MDEA aqueous solution.

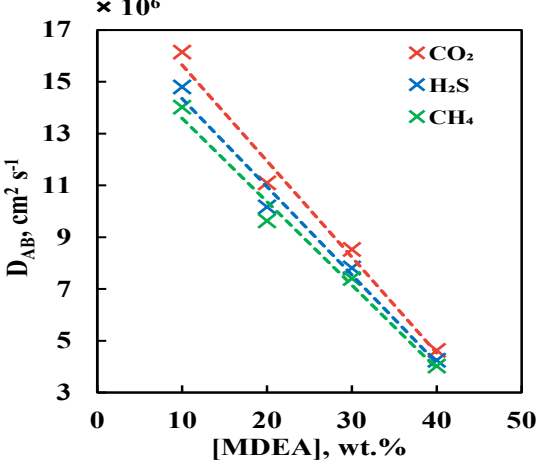


Figure 4 The ideal gas diffusion coefficient in MDEA aqueous solution in dependence of MDEA content for CO<sub>2</sub> loaded absorbent

# 3.2. Determination of the permeance

According to the results of the study for hollow fiber membranes PSF and PEI + PI, the permeance values for a number of gases included in the considered gas mixtures were determined, and the results are shown in Supplementary Tables S2–S5. The polysulfone hollow fiber has higher permeance values for all the considered gases. Thus, for the polysulfone membrane, the permeance decreases in the series  $CO_2 > H_2S > C_4H_{10} > CH_4 > C_2H_6 > N_2 > C_3H_8 > Xe$  and are 322.1, 244.3, 37.2, 30, 22.9, 22.3, 16.9, and 11.2 GPU, respectively. Simultaneously, the PEI+PI membrane permeance values decrease in the series  $CO_2 > H_2S > CH_4 > C_2H_6 = C_3H_8 = C_4H_{10} > N_2 > Xe$  and are 30.7, 13.6, 2.8, 2, 2, 2, 1.6, and 0.9 GPU, respectively. Thus, the PEI+PI membrane's permeance values are lower than those of the PSF membrane by more than 90.5 %. Simultaneously, both membranes demonstrate comparable selectivity values.

Studying the gas transport characteristics of the components of the gas mixture, the permeance values of the PEI+PI membrane for all of the considered components practically do not change. A sharp increase in values is observed for the PSF membrane, which is most likely caused by the plasticization of the membrane under the influence of carbon dioxide and hydrogen sulfide. Simultaneously, there is a significant decrease in membrane selectivity for all considered gas pairs. However, such values are retained during the membrane's long-term operation. Since membrane permeance is the key characteristic determining the possibility of its application in the membrane-assisted gas absorption technique, polysulfone fibers are the most preferable option.

Furthermore, the mass transfer properties of the membrane-assisted gas absorption cell were studied. The assembled cell was connected to a permeance experimental setup coupled with a residual gas analyzer. The connection was performed according to the scheme given in Figure1 except for the helium sweep inlet. It was stubbed, and the permeate outlet was connected to the permeance test setup's vacuum line.

**Table 5** Mass transfer properties of the membrane-assisted gas absorption cell based on hollow PSF fibers

Q, GPU <sup>a</sup>									
$N_2$	CH <sub>4</sub>	Xe	$C_2H_6$	$C_3H_8$	$C_4H_{10}$	$CO_2$	$H_2S$		
0.02	0.03	-	0.02	0.02	0.02	6.2	4.2		
$\alpha (CO_2/x)$									
CH <sub>4</sub>	$C_2H_6$		$C_3H_8$	$C_4H_{10}$	$N_2$		$H_2S$		
206.67	310.00		310.00	310.00	310	.00	1.48		
$\alpha (H_2S/x)$									
$CH_4$	$C_2H_6$		$C_3H_8$	$C_4H_{10}$	N	2	$CO_2$		
140.00	210.00		210.00	210.00	210	.00	0.68		
	6 400 1 D	- 00							

<sup>@</sup> pressure drop of 400 kPa, 25 °C.

 $<sup>^{</sup>a}1 \text{ GPU} = 1 \times 10^{-6} \text{ cm}^{3} \text{ cm}^{-2} \text{ s}^{-1} \text{ cm Hg}^{-1}$ 

As a result of the comparison of the mass transfer characteristics between the combined membrane-assisted gas absorption system and supported ionic liquids (IL) membranes (Table 6), as another class of barrier with a liquid layer, the system under study is characterized by moderate permeability values. Thus, the CO<sub>2</sub> permeability of the system under consideration is 6.2 GPU, which is higher than the value obtained for porous aluminum oxide with phenolic resin and [EMIM][BF<sub>4</sub>] (0.182 GPU) but lower than the same value for other SILMs. At the same time, the system under study achieves the highest selectivity for CO<sub>2</sub>/N<sub>2</sub> and CO<sub>2</sub>/CH<sub>4</sub> pairs. Comparison for H<sub>2</sub>S/N<sub>2</sub> and H<sub>2</sub>S/CH<sub>4</sub> pairs seems impossible because there are no data for liquid membranes. From the presented values of the mass transport characteristics of the combined system, it is evident that the permeability of that system is many times lower than that of a membrane, especially when exposed to hydrogen sulfide. Simultaneously, the system selectivity increases significantly, which is associated with the use of an absorption solution.

**Table 6** Comparison of the mass transfer properties of the membrane-assisted gas absorption cell with supported ionic liquid membranes

11	1							
Crystom	Q, GPU			α				
System	$CH_4$	$N_2$	$CO_2$	$H_2S$	$CO_2/CH_4$	$CO_2/N_2$	$H_2S/CH_4$	$H_2S/N_2$
Present study*	0.03	0.02	6.2	4.2	206.67	310.00	210.00	210.00
Nanoporous aluminum with [BMIM][Ac]**			54			5.4		
Porous aluminum oxide + phenolic resin with [EMIM][BF <sub>4</sub> ]**			0.182			40		
Graphene oxide with [BMIM][BF <sub>4</sub> ]**			68.5		234	382		
Polyimide P-84 with [APTMS][Ac]**			23		41			
γ-alumina and [EMIM][FAP]**			208		3			

<sup>\* - @</sup> pressure drop of 400 kPa, 25 °C.

# 3.3. Performance test of the membrane-assisted gas absorption unit

### 3.1.1. <u>Separation of the model gas mixture</u>

The efficiency of the proposed technique during natural gas processing was evaluated on the example of two gas mixtures: a three-component mixture containing methane, carbon dioxide, and xenon at a ratio of 94.5/5.35/0.15 vol.% and an eight-component mixture containing methane, ethane, carbon dioxide, propane, nitrogen, butane, hydrogen sulfide, and xenon at a ratio of 75.67/7.41/5.396/4.534/3.013/2.469/1.389/0.113 vol.%. A 30 wt.% aqueous solution of amino alcohol - methyldiethanolamine was used as the absorbent. Figures 5 and 6 show the results obtained for the separation process of the three-component gas mixture. Figure5 contains data on the dependence of the ternary gas mixture content in the retentate flow on the stage-cut. Figure6 shows the dependence of the methane and carbon dioxide content in the permeate flow on the stage cut. The dependence of xenon content in the permeate flow on the stage-cut is not shown, as its content was below the detection limit of the gas chromatograph equipped with a thermal conductivity detector with increased sensitivity in the whole range of stage-cut value. Thus, we can conclude that the xenon content in the permeate stream did not exceed 10 ppm.

From the presented dependence of methane concentration on the stage-cut (Figure 5a), when the process is carried out with the minimum value of the stage-cut, no change in the composition of the separated mixture is observed. Therefore, the methane concentration in a retentate stream is 94.59

<sup>\*\*</sup> Literature data (Friess et al., 2021)

vol.%; thus, its initial concentration in a mix was equal to 94.5 vol.%. However, the maximum achieved concentration of this component in the retentate flow is 98.8 vol.%. It is evident from the presented dependence that the growth of stage-cut is accompanied by a significant growth of methane content in retentate flow. Such dependence is explained by the fact that methane is a low-soluble component in the used absorption system, as well as by the fact that the membrane permeability value for this component is significantly lower than that for carbon dioxide. Since the stage-cut is determined by the ratio of the permeate flow rate to the feed flow rate, increasing the stage-cut means increasing the permeate flow rate (if the feed flow rate is constant). Thus, when the stage-cut increases, a more soluble component, i.e., carbon dioxide, permeates the combined membrane-absorbent system, allowing the retentate flow to obtain more concentrated methane.

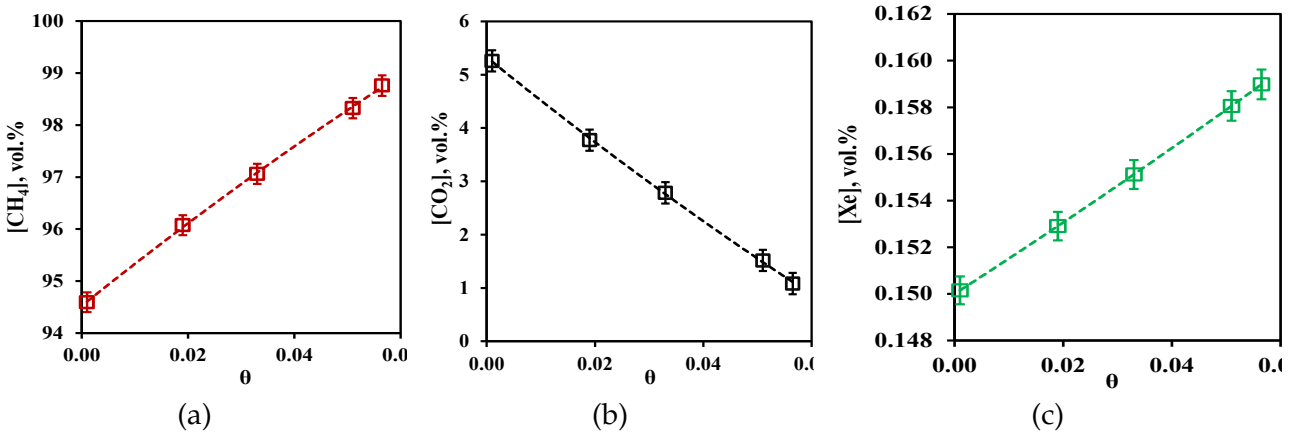


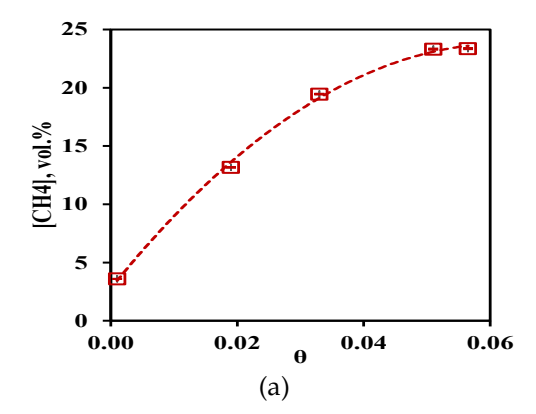
**Figure 5** Dependence of the methane (a), carbon dioxide (b), and xenon (c) contents in the retentate flow on the stage-cut during the separation of a three-component gas mixture using a membrane-assisted gas absorption unit

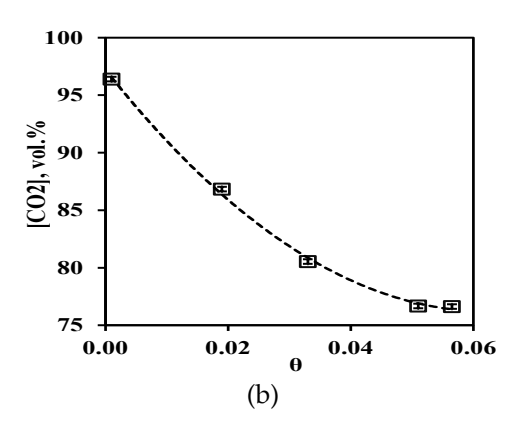
The dependence of the carbon dioxide content in the retentate flow on the stage-cut, presented in Figure 5b, is in good agreement with the conclusions described above. The growth of the stage-cut is accompanied by a sharp decrease in carbon dioxide content in the retentate stream. Therefore, at the minimum stage-cut value, the carbon dioxide concentration is equal to 5.26 vol.% at its initial content of 5.35 vol.%. Thus, performing the process at the maximum stage-cut value allows the concentration of carbon dioxide in the retentate flow to be reduced to 1.08 vol.%. Such dependence is explained by the fact that carbon dioxide is soluble in the used absorption system, and its efficient removal from the system at a higher permeate flow rate allows it to be removed from the separated gas mixture.

Figure 5c shows the stage-cut dependence of the xenon content in the retentate flow. The curve describing this dependence shows that the growth of the stage-cut value is accompanied by a slow increase in xenon concentration in the withdrawn flow. In this case, the process at the lowest value of the stage-cut maintains the initial xenon concentration. However, a further increase in the stage-cut practically does not affect the change in xenon concentration in the retentate flow. This dependence is explained by two factors: the ability of xenon to dissolve in water, the low permeability of the membrane used, and the relatively large kinetic diameter of the xenon molecule. Thus, the reduction of xenon concentration in the retentate flow compared to its content in the feed is most likely because some of it is dissolved in the liquid absorbent's water. Simultaneously, the low membrane permeability to this component and the large size of the molecule do not allow xenon to permeate through the combined membrane-absorbent system. This explains why the xenon content in the permeate stream was below the GC detection limit. The increase in the xenon concentration observed with the increase in the stage-cut is due to the solubility limit for this component being reached in the membrane-absorber module, which simultaneously leads to some loss of this component in the absorbent. However, the xenon does not permeate the submembrane

space, indicating that these losses are not irreversible. Thus, the regeneration of the absorbent will allow the extraction of the dissolved xenon. This effect should be considered in the further optimization of the proposed technique.

Figure 6a shows the stage-cut dependence of methane concentration in the permeate flow during separation of a three-component gas mixture. The curve shows that the growth of the stage-cut is accompanied by an increase in the methane concentration in the permeate stream. Therefore, at the lowest stage-cut value, the methane concentration is equal to 3.6 vol.%, and at stage-cut values of 0.05 and 0.06, the methane content in the permeate stream is 23.32 and 23.37 vol.%, respectively. A change in the stage-cut from 0.05 to 0.06 is not accompanied by a significant change in the methane concentration in the permeate stream, whereas the change in the stage-cut from 0.02 to 0.03 causes a sharp increase in the methane content in this stream. The dependence obtained for the permeate flow is in good agreement with the data obtained for the retentate flow. Thus, an increase in the stage-cut and, consequently, the permeate flow rate leads to an increase in the fraction of methane permeating through the combined membrane-absorbent system. Since methane is practically insoluble in the absorbent used, the diffusion processes is the most likely cause of gas transfer through the system. Such an effect requires an additional study to determine the diffusion coefficients of the gases included in the mixtures.





**Figure 6** Dependence of methane content in the permeate flow on the stage-cut during the separation of a three-component gas mixture using a membrane-assisted gas absorption unit

Figure 6b illustrates the dependence of the carbon dioxide content in the permeate flow on the stage-cut, at which the membrane-assisted gas absorption unit is separated.

The curve shown in the figure shows that the increase in the stage-cut in the whole observed range is accompanied by a change in the carbon dioxide content from 96.4 to 76.6 vol.%. At the same time, the concentration of carbon dioxide does not fall below 76.6 vol.%, which allows us to make a conclusion about the high efficiency of the proposed technique, because the conventional membrane gas separation rarely allows to obtain a carbon dioxide concentrate of more than 50 - 65 vol.% in one stage even when using a highly selective membrane (Merkel et al., 2010).

As a result of the cumulative analysis of the obtained results on the example of separation of a three-component gas mixture, the proposed technique is promising for the task of removing acid gases from the natural gas flow. Thus, the maximum purity of methane withdrawn in the form of retentate flow is 98.8 vol.% at the same content in the permeate flow at a level ~ 24 vol.%. Optimization of the process is required to reduce methane losses in the permeate stream, aimed at selecting the most effective absorbent solution. Its selective adsorption reduces the transfer of methane into the submembrane space.

## 3.1.2. Separation of the quasi-real mixture

A similar study was conducted for an eight-component gas mixture containing methane, ethane, carbon dioxide, propane, nitrogen, butane, hydrogen sulfide, and xenon in the ratio: 75.677/7.41/5.396/4.534/3.013/2.469/1.389/0.113 mol% for a more detailed and approbation of

the proposed technique. Figures 8 and 9 show the results of the separation of the quasi-real gas mixture. Figure 7 shows the retentate stream composition as a function of stage-cut. Figure 8 presents data on the composition of the stage-cut permeate stream. Similar to the previous case, data on xenon in both streams are not provided because its content is below the detection limit of the gas chromatograph, even though a thermal conductivity detector with increased sensitivity was used. Based on this, the xenon content in the permeate does not exceed 10 ppm.

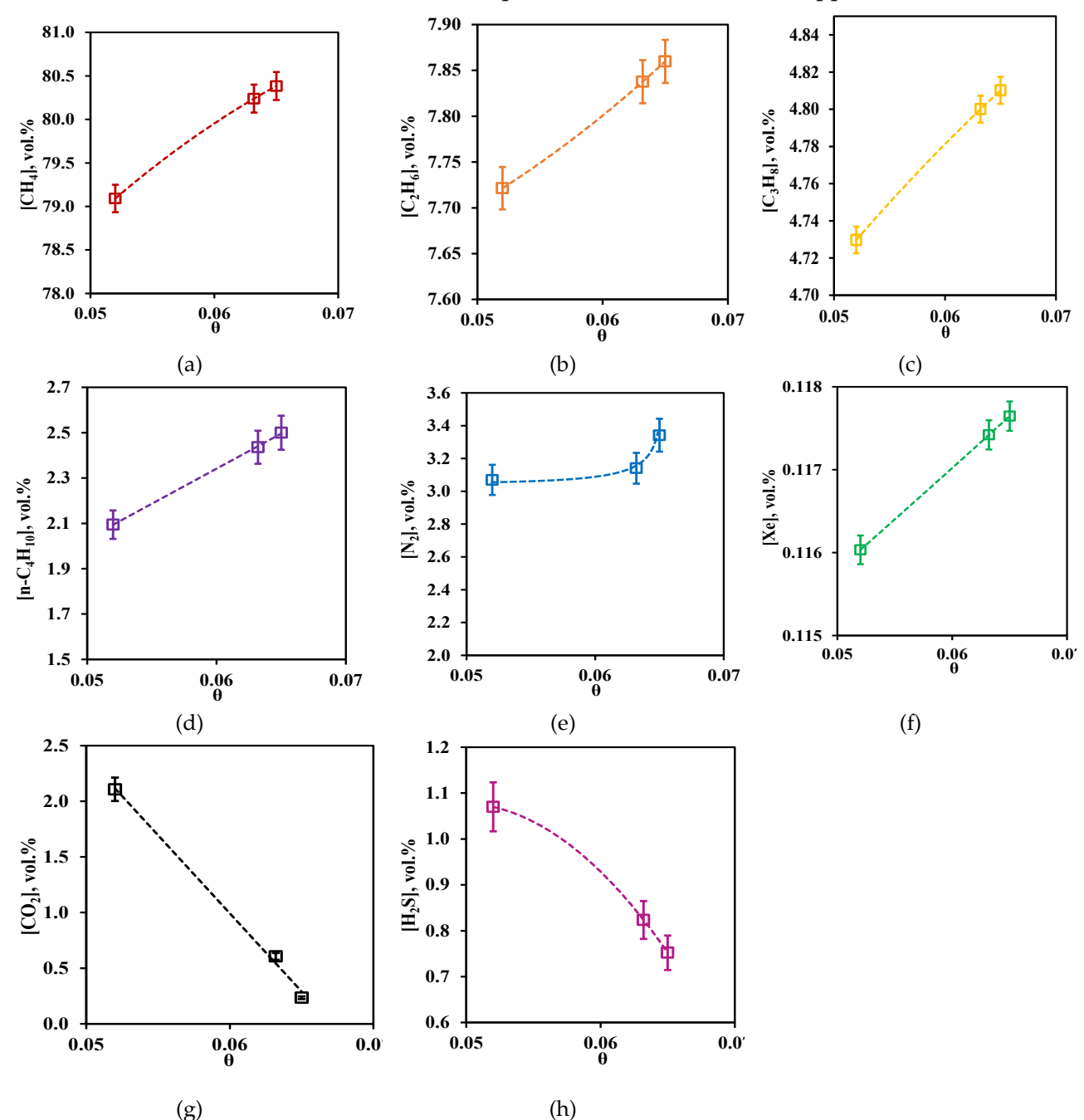


**Figure 7** - Dependence of methane (a), ethane (b), propane (c), n-butane (d), nitrogen (e), xenon (f), carbon dioxide (g), and hydrogen sulfide (h) contents in the retentate flow on the stage-cut during the separation of an eight-component gas mixture using a membrane-assisted gas absorption unit

Figure 7a shows the dependence of methane concentration in the retentate flow on the stage-cut. From the presented curve, it is evident that the change in methane content is in the range of 79.1–80.4 vol.%, indicating an insignificant change in this value from the stage-cut at which the process

is realized. Given the initial content of this component in the mixture (75.677 vol.%), the membrane-assisted gas absorption process contributes to an insignificant concentration of methane in the withdrawn flow. In this case, an increase in the stage-cut is accompanied by an increase in the methane concentration value, which is in good agreement with the data obtained earlier for the three-component gas mixture. The obtained dependence is explained by the fact that an increase in the permeate flow rate is causing the stage-cut growth. This, in turn, contributes to the efficient removal of soluble components to the permeate side. Since methane is practically insoluble in the selected absorbent, its buildup occurs in the retentate flow.

Figure 7b shows the dependence of the ethane content in the retentate flow on the stage cut, at which the gas separation process is realized. From the presented dependence, it can be seen that the concentration of ethane, as well as in the case of methane, practically does not depend on the stage-cut value. Thus, as the stage-cut growth progresses, the content of this component in the retentate stream becomes insignificant, i.e., the ethane concentration increases from 7.72 to 7.86 vol. % when the stage cut was changed from 0.05 to 0.065. Since ethane is also a low-soluble component, its concentration depends insignificantly on the gas flow rate passing through the combined membrane-absorbent system. Comparing the concentration of ethane in the feed flow with its initial content in the mixture (7.41 vol.%), an insignificant concentration of this component was observed.

Figure 7c shows the dependence of the stage-cut propane content in the retentate stream. This curve shows that the tendency described above for other hydrocarbons is also observed for propane. Therefore, at the stage-cut value of 0.05, the propane content in the permeate stream is 4.73 vol.%. At the maximum value of the stage-cut (0.065), its concentration is 4.81 vol.%. Here, it is necessary to note that as a result of carrying out the process even at the lowest value of the stage-cut, which promotes the least concentration of hardly permeable and low-soluble components, the growth of the propane content equal to 0.2 vol.% is observed in comparison with its initial content.

Figure 7d illustrates the dependence of the n-butane concentration in the retentate flow on the stage cut. From the obtained dependence, it can be seen that in this case, the change in stage-cut causes a more pronounced change in the content of this component in the retentate flow than in the case of ethane and propane. Thus, carrying out the process at the stage-cut equal to 0.05, a decrease in the n-butane concentration value ( $\sim 2.1 \text{ vol.\%}$ ) is observed in comparison with its initial content in the mixture (2.469 vol.%). However, an increase in the stage-cut to 0.065 is accompanied by an increase in the n-butane concentration to 2.5 vol.%, which is equal to its initial content. Thus, the cumulative analysis of the dependencies of hydrocarbon concentrations on the value of the stage-cut shows that insignificant concentration change is observed for all these components when the stage-cut value  $\geq 0.06$ . Thus, the application of a hybrid membrane-assisted gas absorption method allows the concentration of these components in the retentate stream.

Figure 7e shows the dependence of the stage-cut nitrogen content in the retentate flow. The obtained dependence shows that the nitrogen content in the captured retentate stream does not depend on the stage-cut value at which the gas separation process is implemented. Thus, the nitrogen concentration in the whole considered range of stage-cut values varies from 3.1 to 3.34 vol.%. Simultaneously, comparing the achieved nitrogen concentration with its initial content in the separated gas mixture, its content increased by 0.33 vol.%. Thus, we can conclude that the implementation of the membrane-assisted gas absorption process allows for a slight concentration of nitrogen, which is also a low-soluble component unable to permeate and concentrate on the permeate side.

Figure 7f illustrates the dependence of the stage-cut value on the xenon content in the retentate flow. In general, a dependence similar to that of nitrogen is observed for xenon. In the whole considered range of the stage-cut, the xenon concentration value varies from 0.116 to 0.117 vol.%. However, there is a weak tendency of an increase in xenon concentration with an increase in the stage-cut, at which the gas separation process is realized. Thus, at a stage-cut of 0.05, the xenon concentration is equal to 0.116 vol.%, and at a stage-cut of 0.065, the xenon concentration decreases to 0.117 vol.%. A linear dependence of Xe content on stage-cut is observed. The dependence

obtained for the eight-component mixture is in good agreement with the dependence obtained for the ternary mixture. Although xenon can dissolve in the water contained in the liquid absorbent used, this does not occur in the absence of other components (nitrogen, ethane, propane, n-butane, hydrogen sulfide) in the triple mixture. The specific sorption in the presence of hydrogen sulfide most likely explains this dependence, an even more soluble gas. Presumably, the solubility limit is reached in the membrane-assisted gas absorption unit, which does not allow xenon to sorb in a liquid saturated with more soluble components-carbon dioxide and hydrogen sulfide.

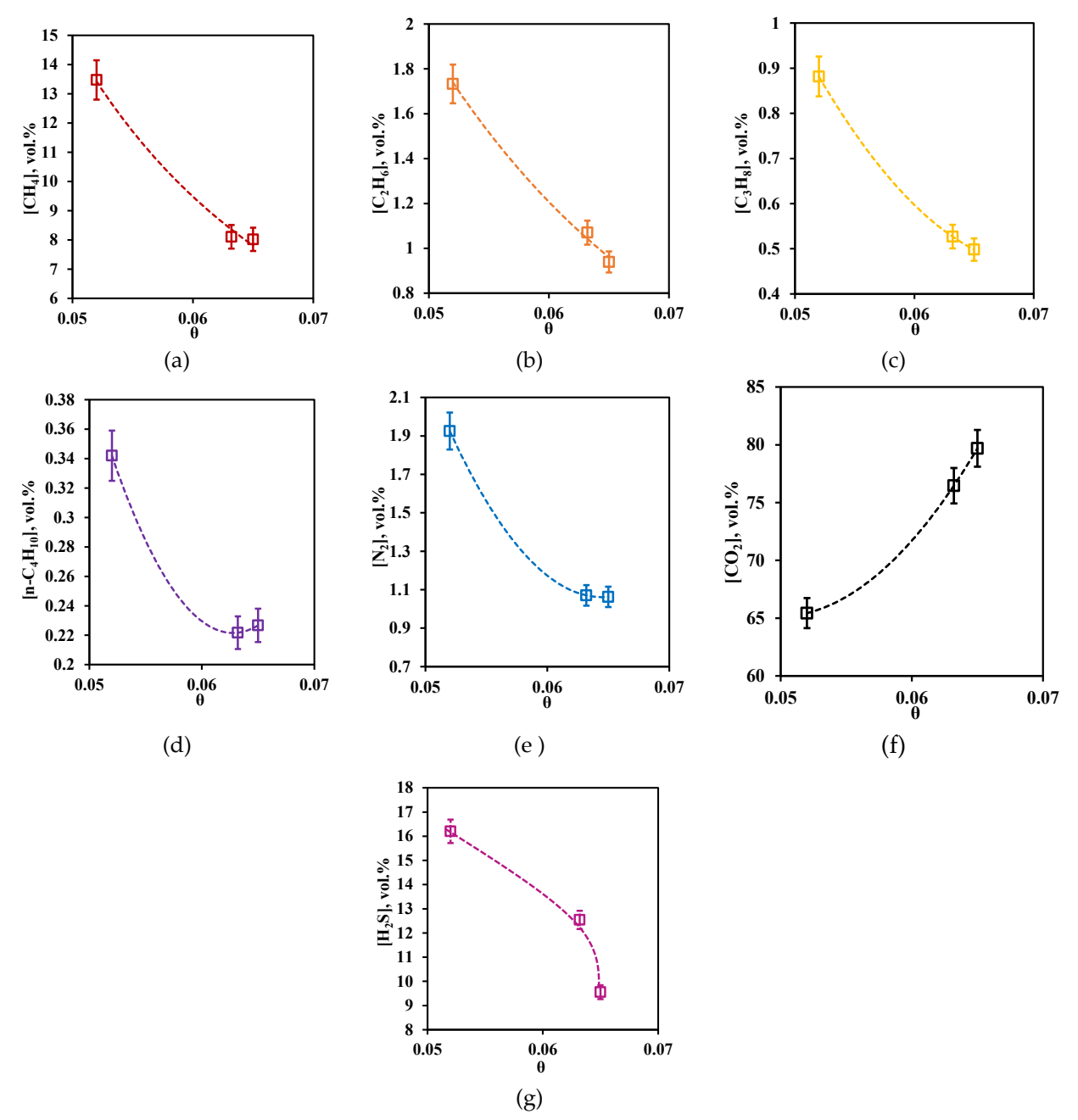
Figure 7g shows the dependence of the stage-cut carbon dioxide content in the retentate flow. The obtained dependence shows that an increase in the stage-cut is accompanied by a decrease in the retentate stream's carbon dioxide content, which is withdrawn from the membrane-assisted gas absorption module. Thus, the maximum concentration of carbon dioxide is 2.1 vol.% at a stage cut of 0.05. The carbon dioxide content decreases to 0.23 vol.% when performing the separation process at the stage-cut of 0.065. At the same time, there is a significant decrease in the carbon dioxide concentration compared with its initial content in the mixture (5.396 vol.%). Thus, at a stage-cut of 0.05, the carbon dioxide concentration decreases by 3.3 vol.%, and at a process stage-cut value of 0.065, the carbon dioxide concentration decreases by 5.17 vol.%. The obtained dependence is explained by the fact that carbon dioxide is well dissolved in the liquid absorbent used, and the membrane is characterized by the highest permeability by this component (among the components of the mixture). Thus, in the process under consideration, carbon dioxide is able to dissolve effectively in the liquid absorbent layer and move into the submembrane space of the membrane-assisted gas absorption unit.

Figure 7h presents the dependence of hydrogen sulfide concentration on the stage-cut value at which the separation process is carried out. The received curve shows that the growth of the stage-cut is accompanied by a decrease in hydrogen sulfide content in a retentate stream. Thus, at a stage-cut of 0.05, the hydrogen sulfide concentration is 1.07 vol.%, and at a stage-cut of 0.065, the hydrogen sulfide concentration is 0.75 vol.%. As a result of this process, a decrease in the hydrogen sulfide content compared with its initial concentration in a mix from 0.32 to 0.64 vol.% is observed. Similar to the case of carbon dioxide, the obtained dependence is explained by the absorbent ability to effectively dissolve this component and the relatively high membrane permeance to hydrogen sulfide, which effectively transfers this gas to the permeate side. Thus, implementation of the process at the stage-cut value equal to 0.65, the gas stream withdrawn as retentate consists of methane, ethane, carbon dioxide, propane, nitrogen, n-butane, hydrogen sulfide, and xenon in the ratio 80. 39/7.86/0.23/4.81/3.34/2.50/0.75/0.12 vol.%, which corresponds to an increase in the concentration of all components except impurities of acid gases, and, equally importantly, preservation and a slight increase in xenon content.

Analyzing the composition of the permeate flow at different stage-cut values, the dependences of the concentrations of methane, ethane, propane, n-butane, and nitrogen (Figure 8) on the stage-cut form curves of similar character and similar intensity of concentration decrease, accompanying the increase of the stage-cut value. Therefore, in the process of increasing the stage-cut from 0.05 to 0.065, a decrease in the concentration of these components from 54.2% to 66.3 % from the value received for the stage-cut equal to 0.05 is observed. In absolute values, this corresponds to the following values: 8.02, 0.94, 0.49, 0.23, and 1.06 vol.% for methane, ethane, propane, n-butane, and nitrogen when the stage-cut is equal to 0.065. An explanation of the obtained dependencies is given above. All these components are low-soluble components of a mixture that causes low efficiency of their transfer through the combined membrane-absorbent system. Consequently, their low content in a permeate stream corresponds to small losses on these components even at high value of the stage-cut at which the considered gas separation process is realized.

Figure 8f and 8g show the dependence of the stage-cut on the concentration of impurities of acid gases, i.e., carbon dioxide and hydrogen sulfide, in the permeate flow. The presented curves show that the character of these dependences is opposite, but the concentration values of these components are high. Therefore, the concentration of carbon dioxide is in a range 65.43 - 79.7 vol.%,

and the hydrogen sulfide content in the permeate stream is 9.55 - 16.21 vol.%. For carbon dioxide there is a significant growth in its concentration caused by the growth of the stage-cut. At the transition of a value of the stage-cut from 0.052 to 0.06, the concentration of carbon dioxide increases by 11 vol.%, and at the cut increase to 0.065, the concentration of carbon dioxide increases by 14.27 vol.%. Decrease in hydrogen sulfide concentration in a permeate stream caused by increase of the stage-cut is less intensive and makes 3.66 and 2.99 vol.% at the same step increase of the stage-cut value. Thus, performing the membrane-assisted gas absorption process at the stage-cut equal to 0.065 (which corresponds to the most effective concentration of hydrocarbons in the retentate stream) allows a permeate stream enriched with acid gases to be received. The composition of such flow corresponds to the following proportions of methane, ethane, carbon dioxide, propane, nitrogen, n-butane, hydrogen sulfide 8.02/0.94/79.7/0.5/1.06/0.23/9.55 vol.%:



**Figure 8** Dependence of methane (a), ethane (b), propane (c), n-butane (d), nitrogen (e), carbon dioxide (f), and hydrogen sulfide (g) contents in the permeate flow on the stage-cut during the separation of an eight-component gas mixture using a membrane-assisted gas absorption unit

The ultimate efficiency of the considered process represented as the amount of acid gases removed is 96% and 61 % of carbon dioxide and hydrogen sulfide, respectively. Under the same conditions, the hydrocarbon losses were up to 0.95 %. In this way, the residual sum of acid gas content may be lowered to 0.99 vol.% from 6.79 vol.% in one stage using the heat-free hybrid membrane-assisted gas absorption technique while maintaining a suitable methane, ethane, propane, and n-butane recovery rate. The acid gas content in the processed gas stream meets the limitations indicated in the Russian Government Standard GOST 5542-2022 (GOST, 2022). Nevertheless, the overall efficiency of the process may be enhanced using the specific absorption agents with aqueous amino alcohol solutions.

#### 4. Conclusions

This study continues the development and investigation of the MAGA method. The possibility of improving the efficiency of the system by optimizing the cell configuration was discussed. Optimization of the configuration involves the use of two types of hollow fibers, which reduces the ratio between the absorbent volume and the membrane area. The complexity of the approach to evaluate the efficiency of the membrane-assisted gas absorption process is stated by considering two gas mixes: ternary model mix and quasi-real natural gas. The present experimental study of the novel heat-free process in natural gas sweetening application showed that the sum of acid gas content may be lowered to less than 1 vol.% in one stage in a continuous mode without any pumping gear and specific absorbent regeneration step. The composition of the product stream is methane, ethane, carbon dioxide, propane, nitrogen, n-butane, hydrogen sulfide, and xenon in the ratio 80.39/7.86/0.23/4.81/3.34/2.50/0.75/0.12 vol.%. In this way, the ultimate efficiency of the considered process represented as the amount of acid gases removed is 96% and 61 % of carbon dioxide and hydrogen sulfide, respectively. Taking into account many variations in the composition of natural gas, for example, the higher acid gas content, the membrane-assisted gas absorption process may be tuned by increasing the membrane area, absorbent composition, and its content to achieve the desired result. Moreover, the typical requirement for the CO2 content in natural gas supplied to the pipeline is less than 2 %, whereas the proposed technique allows it to be decreased to 0.23 % with minimal loss of valuable hydrocarbons. Nevertheless, the overall efficiency of the process may be enhanced using specific absorption agents with aqueous amino alcohol solutions. Ionic liquids, piperazine, and other alkanolamines, for example, are used as additives that increase the sorption capacity of such solutions. Further study will be devoted to the appliance of novel absorbent systems, based on «green» and cheap ionic liquids, which will increase the absorption capacity of alkanolamine aqueous solutions.

# Acknowledgements

The main part of the study was supported by the Russian Science Foundation (project no. 22-79-10222). The analytical support was funded by The Ministry of Science and Higher Education of the Russian Federation within the framework of the scientific project of the laboratory «Laboratory of Electronic Grade Substances Technologies», project No. FSSM2022-0005. Mass-transfer properties of the combined membrane-absorbent systems were study was funded by Ministry of Science and Education of the Russian Federation within the framework of the scientific project No. FSSM-2023-0004.

# **Author Contributions**

Conceptualization, A.N. Petukhov; Software, D.M. Zarubin; Formal analysis, S.S. Suvorov; Investigation, K.A. Smorodin.; Data curation, M.E. Atlaskina and E.A. Stepanova.; Methodology, A.A. Atlaskin, O.V. Kazarina; Writing—original draft, S.S. Kryuchkov and A.A. Atlaskin.; Visualization, A.N. Stepakova.; Validation, A.V. Vorotyntsev; Supervision, I.V. Vorotyntsev. All authors have read and agreed to the published version of the manuscript.

#### Conflict of Interest

The authors have no conflicts of interest to declare.

#### References

Atlaskin, AA, Kryuchkov, SS, Smorodin, KA, Markov, AN, Kazarina, OV, Zarubin, DM, Atlaskina, ME, Vorotyntsev, AV, Nyuchev, AV, Petukhov, AN & Vorotyntsev, IV 2021, 'Towards the potential of trihexyltetradecylphosphonium indazolide with aprotic heterocyclic ionic liquid as an efficient absorbent for membrane-assisted gas absorption technique for acid gas removal applications', *Separation and Purification Technology*, vol. 257, article 117835, <a href="https://doi.org/10.1016/j.seppur.2020.117835">https://doi.org/10.1016/j.seppur.2020.117835</a>

Atlaskin, AA, Kryuchkov, SS, Yanbikov, NR, Smorodin, KA, Petukhov, AN, Trubyanov, MM, Vorotyntsev, VM & Vorotyntsev, IV 2020, 'Comprehensive experimental study of acid gases removal process by membrane-assisted gas absorption using imidazolium ionic liquids solutions absorbent', *Separation and Purification Technology*, vol. 239, article 116578, <a href="https://doi.org/10.1016/j.seppur.2020.116578">https://doi.org/10.1016/j.seppur.2020.116578</a>

Bashir, Z, Lock, SSM, Hira, NE, Ilyas, SU, Lim, LG, Lock, ISM, Yiin, CL & Darban, MA 2024, 'A review on recent advances of cellulose acetate membranes for gas separation', *RSC Advances*, vol. 14, no. 31, pp. 19560–19580, <a href="https://doi.org/10.1039/d4ra01315h">https://doi.org/10.1039/d4ra01315h</a>

Bello, MO & Solarin, SA 2022, 'Searching for sustainable electricity generation: The possibility of substituting coal and natural gas with clean energy', *Energy and Environment*, vol. 33, no. 1, pp. 64–84, <a href="https://doi.org/10.1177/0958305x20985253">https://doi.org/10.1177/0958305x20985253</a>

Berchiche, A, Guenoune, M, Belaadi, S & Léonard, G 2023, 'Optimal energy integration and off-design analysis of an amine-based natural gas sweetening unit', *Applied Sciences*, vol. 13, no. 11, article 6559, <a href="https://doi.org/10.3390/app13116559">https://doi.org/10.3390/app13116559</a>

Darani, NS, Behbahani, RM, Shahebrahimi, Y, Asadi, A & Mohammadi, AH 2021, 'Simulation and optimization of the acid gas absorption process by an aqueous diethanolamine solution in a natural gas sweetening unit', ACS Omega, vol. 6, no. 17, pp. 12072–12080, <a href="https://doi.org/10.1021/acsomega.1c00744">https://doi.org/10.1021/acsomega.1c00744</a>

Davarpanah, E, Hernández, S, Latini, G, Pirri, CF & Bocchini, S 2020, 'Enhanced CO<sub>2</sub> absorption in organic solutions of biobased ionic liquids', *Advanced Sustainable Systems*, vol. 4, no. 1, article 1900067, <a href="https://doi.org/10.1002/adsu.201900067">https://doi.org/10.1002/adsu.201900067</a>

Dawodu, OF & Meisen, A 1994, 'Solubility of carbon dioxide in aqueous mixtures of alkanolamines', *Journal of Chemical and Engineering Data*, vol. 39, no. 3, pp. 548–552, <a href="https://doi.org/10.1021/je00015a034">https://doi.org/10.1021/je00015a034</a> Ellaf, A, Taqvi, SAA, Zaeem, D, Siddiqui, FUH, Kazmi, B, Idris, A, Alshgari, RA & Mushab, MSS 2023, 'Energy, exergy, economic, environment, exergo-environment based assessment of amine-based hybrid solvents for natural gas sweetening', *Chemosphere*, vol. 313, article 137426, <a href="https://doi.org/10.1016/j.chemosphere.2022.137426">https://doi.org/10.1016/j.chemosphere.2022.137426</a>

Friess, K, Izák, P, Kárászová, M, Pasichnyk, M, Lanč, M, Nikolaeva, D, Luis, P & Jansen, JC 2021, 'A review on ionic liquid gas separation membranes', *Membranes*, vol. 11, no. 2, article 97, <a href="https://doi.org/10.3390/membranes11020097">https://doi.org/10.3390/membranes11020097</a>

Fu, D, Zhang, P & Mi, CL 2016a, 'Effects of concentration and viscosity on the absorption of CO<sub>2</sub> in [N1111][Gly] promoted MDEA (methyldiethanolamine) aqueous solution', *Energy*, vol. 101, pp. 288–295, <a href="https://doi.org/10.1016/j.energy.2016.02.052">https://doi.org/10.1016/j.energy.2016.02.052</a>

Fu, D, Zhang, P & Wang, LM 2016b, 'Absorption performance of CO2 in high concentrated [Bmim][Lys]-MDEA aqueous solution', *Energy*, vol. 113, pp. 1–8, <a href="https://doi.org/10.1016/j.energy.2016.07.049">https://doi.org/10.1016/j.energy.2016.07.049</a>

Ghasem, N 2020, 'CO<sub>2</sub> removal from natural gas', *Advances in Carbon Capture: Methods, Technologies and Applications*, pp. 479–501, <a href="https://doi.org/10.1016/b978-0-12-819657-1.00021-9">https://doi.org/10.1016/b978-0-12-819657-1.00021-9</a>

Godin, J, Liu, W, Ren, S & Xu, CC 2021, 'Advances in recovery and utilization of carbon dioxide: A brief review', *Journal of Environmental Chemical Engineering*, vol. 9, no. 4, article 105644, https://doi.org/10.1016/j.jece.2021.105644

GOST 2022, 'Natural gas for industrial and municipal purposes. Technical conditions', GOST 5542-2022, *Internet Law*, viewed 14 August 2024, (<a href="https://internet-law.ru/gosts/gost/77776/">https://internet-law.ru/gosts/gost/77776/</a>)

Hadri, NEL, Quang, DV & Abu-Zahra, MRM 2015, 'Study of novel solvent for CO2 post-combustion capture', *Energy Procedia*, vol. 75, pp. 2268–2286, <a href="https://doi.org/10.1016/j.egypro.2015.07.414">https://doi.org/10.1016/j.egypro.2015.07.414</a>

Hazarika, G & Ingole, PG 2024, 'Polymer-based hollow fiber membranes: A modern trend in gas separation technologies', *Materials Today Chemistry*, vol. 38, article 102109, <a href="https://doi.org/10.1016/j.mtchem.2024.102109">https://doi.org/10.1016/j.mtchem.2024.102109</a>

Ibrahim, AY, Ashour, FH, Gadalla, MA & Farouq, R 2022, 'Exergy study of amine regeneration unit for diethanolamine used in refining gas sweetening: A real start-up plant', *Alexandria Engineering Journal*, vol. 61, no. 1, pp. 101–112, <a href="https://doi.org/10.1016/j.aej.2021.04.085">https://doi.org/10.1016/j.aej.2021.04.085</a>

Jamal, A, Meisen, A & Lim, CJ 2006, 'Kinetics of carbon dioxide absorption and desorption in aqueous alkanolamine solutions using a novel hemispherical contactor—I. Experimental apparatus and mathematical modeling', *Chemical Engineering Science*, vol. 61, no. 19, pp. 6571–6589, <a href="https://doi.org/10.1016/j.ces.2006.04.046">https://doi.org/10.1016/j.ces.2006.04.046</a>

Jana, A & Modi, A 2024, 'Recent progress on functional polymeric membranes for CO<sub>2</sub> separation from flue gases: A review', *Carbon Capture Science & Technology*, vol. 11, article 100204, https://doi.org/10.1016/j.ccst.2024.100204

Jou, F-Y, Mather, AE & Otto, FD 1995, 'The solubility of  $CO_2$  in a 30 mass percent monoethanolamine solution', *Canadian Journal of Chemical Engineering*, vol. 73, no. 1, pp. 140-147, <a href="https://doi.org/10.1002/cjce.5450730116">https://doi.org/10.1002/cjce.5450730116</a>

Karamah, EF, Arbi, DS, Bagas, I & Kartohardjono, S 2021, 'Hollow fiber membrane modules for NOx removal using a mixture of NaClO3 and NaOH solutions in the shell side as absorbents', *International Journal of Technology*, vol. 12, no. 4, pp. 690–699, <a href="https://doi.org/10.14716/ijtech.v12i4.4408">https://doi.org/10.14716/ijtech.v12i4.4408</a>

Kartohardjono, S, Karamah, EF, Talenta, GN, Ghazali, TA & Lau, WJ 2023, 'The simultaneously removal of NOx and SO2 processes through a polysulfone hollow fiber membrane module', *International Journal of Technology*, vol. 14, no. 3, pp. 576–583, <a href="https://doi.org/10.14716/ijtech.v14i3.5544">https://doi.org/10.14716/ijtech.v14i3.5544</a>

Khan, AU, Hazaraimi, MH, Othman, MHD, Younas, M, Karim, ZA, Tai, ZS, Samuel, O, Puteh, MH, Kurniawan, TA, Wong, KY & Yoshida, N 2024, 'A comprehensive review on dual-layer organic hollow fiber membranes fabrication via co-extrusion: Mechanistic insights, water treatment and gas separation applications', *Journal of Environmental Chemical Engineering*, vol. 12, no. 5, article 112434, <a href="https://doi.org/10.1016/j.jece.2024.112434">https://doi.org/10.1016/j.jece.2024.112434</a>

Khan, IU, Othman, MHD & Jilani, A 2021, 'High performance membrane for natural gas sweetening plants', *Advances in Science, Technology and Innovation*, pp. 59–72, <a href="https://doi.org/10.1007/978-3-030-41295-1">https://doi.org/10.1007/978-3-030-41295-1</a> 5

Kryuchkov, S, Smorodin, K, Stepakova, A, Atlaskin, A, Tsivkovsky, N, Atlaskina, M, Tolmacheva, M, Kazarina, O, Petukhov, A, Vorotyntsev, A & Vorotyntsev, I 2024, 'Membrane air separation process simulation: Insight in modelling approach based on ideal and mixed permeance values', *International Journal of Technology*, vol. 15, no. 5, pp. 1218-1236, <a href="https://doi.org/10.14716/ijtech.v15i5.6987">https://doi.org/10.14716/ijtech.v15i5.6987</a>

Kryuchkov, SS, Petukhov, AN & Atlaskin, AA 2021, 'Experimental evaluation of the membrane-assisted gas absorption technique efficiency using an aqueous solution of PEG-400 for the ammonia capture', *In:* IOP Conference Series: Earth and Environmental Science, vol. 666, article 052071, <a href="https://doi.org/10.1088/1755-1315/666/5/052071">https://doi.org/10.1088/1755-1315/666/5/052071</a>

Lei, L, Bai, L, Lindbråthen, A, Pan, F, Zhang, X & He, X 2020, 'Carbon membranes for CO<sub>2</sub> removal: Status and perspectives from materials to processes', *Chemical Engineering Journal*, vol. 401, article 126084, <a href="https://doi.org/10.1016/j.cej.2020.126084">https://doi.org/10.1016/j.cej.2020.126084</a>

Liang, Y, Kleijn, R, Tukker, A & Voet, Evd 2022, 'Material requirements for low-carbon energy technologies: A quantitative review', *Renewable and Sustainable Energy Reviews*, vol. 161, article 112334, <a href="https://doi.org/10.1016/j.rser.2022.112334">https://doi.org/10.1016/j.rser.2022.112334</a>

Litvinenko, V 2020, 'The role of hydrocarbons in the global energy agenda: The focus on liquefied natural gas', *Resources*, vol. 9, no. 5, article 59, <a href="https://doi.org/10.3390/resources9050059">https://doi.org/10.3390/resources9050059</a>

Liu, G, Zhu, L, Cao, W, Liu, H & He, Y 2021a, 'New technique integrating hydrate-based gas separation and chemical absorption for the sweetening of natural gas with high  $H_2S$  and  $CO_2$  contents', ACS Omega, vol. 6, no. 39, pp. 26180–26190, <a href="https://doi.org/10.1021/acsomega.1c03165">https://doi.org/10.1021/acsomega.1c03165</a>

Liu, Y, Chen, Z, Qiu, W, Liu, G, Eddaoudi, M & Koros, WJ 2021b, 'Penetrant competition and plasticization in membranes: How negatives can be positives in natural gas sweetening', *Journal of Membrane Science*, vol. 627, article 119201, <a href="https://doi.org/10.1016/j.memsci.2021.119201">https://doi.org/10.1016/j.memsci.2021.119201</a>

Liu, Y, Liu, Z, Kraftschik, BE, Babu, VP, Bhuwania, N, Chinn, D & Koros, WJ 2021c, 'Natural gas sweetening using TEGMC polyimide hollow fiber membranes', *Journal of Membrane Science*, vol. 632, article 119361, <a href="https://doi.org/10.1016/j.memsci.2021.119361">https://doi.org/10.1016/j.memsci.2021.119361</a>

Liu, Y, Liu, Z, Morisato, A, Bhuwania, N, Chinn, D & Koros, WJ 2020, 'Natural gas sweetening using a cellulose triacetate hollow fiber membrane illustrating controlled plasticization benefits', *Journal of Membrane Science*, vol. 601, article 117910, <a href="https://doi.org/10.1016/j.memsci.2020.117910">https://doi.org/10.1016/j.memsci.2020.117910</a>

Mahi, MR, Mokbel, I, Negadi, L, Dergal, F & Jose, J 2019, 'Experimental solubility of carbon dioxide in monoethanolamine, or diethanolamine or N-methyldiethanolamine (30 wt%) dissolved in deep eutectic solvent (choline chloride and ethylene glycol solution)', *Journal of Molecular Liquids*, vol. 289, article 111062, https://doi.org/10.1016/j.molliq.2019.111062

Makertihartha, IGBN, Kencana, KS, Dwiputra, TR, Khoiruddin, K, Lugito, G, Mukti, RR & Wenten, IG 2022, 'SAPO-34 zeotype membrane for gas sweetening', *Reviews in Chemical Engineering*, vol. 38, no. 4, pp. 431–450, <a href="https://doi.org/10.1515/revce-2019-0086">https://doi.org/10.1515/revce-2019-0086</a>

Merkel, TC, Lin, H, Wei, X & Baker, R 2010, 'Power plant post-combustion carbon dioxide capture: An opportunity for membranes', *Journal of Membrane Science*, vol. 359, no. 1–2, pp. 126–139, https://doi.org/10.1016/j.memsci.2009.10.041

Nasteka, VI 1996, *New technologies of refinery of high-sulfur and gas condensate*, Nedra, Moskow, pp. 1–106

Niu, Z, He, N, Yao, Y, Ma, A, Zhang, E, Cheng, L, Li, Y, & Li, X 2024, 'Mixed matrix membranes for gas separations: A review', *Chemical Engineering Journal*, vol. 494, article 152912, <a href="https://doi.org/10.1016/j.cej.2024.152912">https://doi.org/10.1016/j.cej.2024.152912</a>

Østergaard, PA, Duic, N, Noorollahi, Y, Mikulcic, H & Kalogirou, S 2020, 'Sustainable development using renewable energy technology', *Renewable Energy*, vol. 146, pp. 2430–2437, <a href="https://doi.org/10.1016/j.renene.2019.08.094">https://doi.org/10.1016/j.renene.2019.08.094</a>

Otvagina, KV, Penkova, AV, Dmitrenko, ME, Kuzminova, AI, Sazanova, TS, Vorotyntsev, AV & Vorotyntsev, IV 2019, 'Novel composite membranes based on chitosan copolymers with polyacrylonitrile and polystyrene: Physicochemical properties and application for pervaporation dehydration of tetrahydrofuran', *Membranes*, vol. 9, no. 3, article 38, <a href="https://doi.org/10.3390/membranes9030038">https://doi.org/10.3390/membranes9030038</a>

Petukhov, AN, Atlaskin, AA, Kryuchkov, SS, Smorodin, KA, Zarubin, DM, Petukhova, AN, Atlaskina, ME, Nyuchev, AV, Vorotyntsev, AV, Trubyanov, MM & Vorotyntsev, IV 2021, 'A highly-efficient hybrid technique – Membrane-assisted gas absorption for ammonia recovery after the Haber-Bosch process', *Chemical Engineering Journal*, vol. 421, article 127726, <a href="https://doi.org/10.1016/j.cej.2020.127726">https://doi.org/10.1016/j.cej.2020.127726</a>

Petukhov, AN, Atlaskin, AA, Smorodin, KA, Kryuchkov, SS, Zarubin, DM, Atlaskina, ME, Petukhova, AN, Stepakova, AN, Golovacheva, AA, Markov, AN, Stepanova, EA, Vorotyntsev, AV & Vorotyntsev, IV 2022, 'An efficient technique for ammonia capture in the Haber–Bosch process loop—Membrane-assisted gas absorption', *Polymers*, vol. 14, no. 11, article 2214, <a href="https://doi.org/10.3390/polym14112214">https://doi.org/10.3390/polym14112214</a>

Rahmani, M, Mokhtarani, B & Rahmanian, N 2023, 'High pressure adsorption of hydrogen sulfide and regeneration ability of ultra-stable Y zeolite for natural gas sweetening', *Fuel*, vol. 343, article 127937, <a href="https://doi.org/10.1016/j.fuel.2023.127937">https://doi.org/10.1016/j.fuel.2023.127937</a>

Rayer, AV, Sumon, KZ, Sema, T, Henni, A, Idem, RO & Tontiwachwuthikul, P 2012, 'Part 5c: Solvent chemistry: Solubility of CO<sub>2</sub> in reactive solvents for post-combustion CO<sub>2</sub>', *Carbon Management*, vol. 3, no. 5, pp. 467–484, https://doi.org/10.4155/cmt.12.47

Robeson, LM 2008, 'The upper bound revisited', *Journal of Membrane Science*, vol. 320, no. 1–2, pp. 390–400, <a href="https://doi.org/10.1016/j.memsci.2008.04.030">https://doi.org/10.1016/j.memsci.2008.04.030</a>

Rochelle, GT 2024, 'Air pollution impacts of amine scrubbing for CO<sub>2</sub> capture', *Carbon Capture Science & Technology*, vol. 11, article 100192, <a href="https://doi.org/10.1016/j.ccst.2024.100192">https://doi.org/10.1016/j.ccst.2024.100192</a>

Shirazi, M, Ghasemi, A & Šimurina, J 2022, 'The impact of the North American shale gas technology on the US' energy security: the case of natural gas', *International Journal of Sustainable Energy*, vol. 41, no. 9, pp. 810–831, <a href="https://doi.org/10.1080/14786451.2021.1979002">https://doi.org/10.1080/14786451.2021.1979002</a>

Si, X, Lu, R, Zhao, Z, Yang, X, Wang, F, Jiang, H, Luo, X, Wang, A, Feng, Z, Xu, J & Lu, F 2022, 'Catalytic production of low-carbon footprint sustainable natural gas', *Nature Communications*, vol. 13, no. 1, article 258, <a href="https://doi.org/10.1038/s41467-021-27919-9">https://doi.org/10.1038/s41467-021-27919-9</a>

Singh, R, Prasad, B & Ahn, YH 2024, 'Recent developments in gas separation membranes enhancing the performance of oxygen and nitrogen separation: A comprehensive review', *Gas Science and Engineering*, vol. 123, article 205256, <a href="https://doi.org/10.1016/j.jgsce.2024.205256">https://doi.org/10.1016/j.jgsce.2024.205256</a>

Smetannikov, VP, Orlov, AN, Malinin, NN & Semenova, OP 2010, 'Method of producing xenon concentrate from natural combustible gas, products of its treatment including man-caused off gases and device to this end (versions)', Patent RU 2,466,086

Struk, M, Kushkevych, I & Vítězová, M 2020, 'Biogas upgrading methods: recent advancements and emerging technologies', *Reviews in Environmental Science and Biotechnology*, vol. 19, no. 4, pp. 651–671, <a href="https://doi.org/10.1007/s11157-020-09539-9">https://doi.org/10.1007/s11157-020-09539-9</a>

Tikadar, D, Gujarathi, AM & Guria, C 2021a, 'Safety, economics, environment and energy based criteria towards multi-objective optimization of natural gas sweetening process: An industrial case study', *Journal of Natural Gas Science and Engineering*, vol. 95, article 104207, <a href="https://doi.org/10.1016/j.jngse.2021.104207">https://doi.org/10.1016/j.jngse.2021.104207</a>

Tikadar, D, Gujarathi, AM, Guria, C & Al Toobi, S 2021b, 'Retrofitting and simultaneous multi-criteria optimization with enhanced performance of an industrial gas-cleaning plant using economic, process safety, and environmental objectives', *Journal of Cleaner Production*, vol. 319, article 128652, <a href="https://doi.org/10.1016/j.jclepro.2021.128652">https://doi.org/10.1016/j.jclepro.2021.128652</a>

Valappil, RSK, Ghasem, N & Al-Marzouqi, M 2021, 'Current and future trends in polymer membrane-based gas separation technology: A comprehensive review', *Journal of Industrial and Engineering Chemistry*, vol. 98, pp. 103–129, <a href="https://doi.org/10.1016/j.jiec.2021.03.030">https://doi.org/10.1016/j.jiec.2021.03.030</a>

Vorotyntsev, IV, Drozdov, PN, Shablikin, DN & Gamajunova, TV 2006a, 'Ammonia separation and purification by absorbing pervaporation', *Desalination*, vol. 200, no. 1–3, pp. 379–380, <a href="https://doi.org/10.1016/j.desal.2006.03.382">https://doi.org/10.1016/j.desal.2006.03.382</a>

Vorotyntsev, VM, Drozdov, PN & Vorotyntsev, IV 2009, 'High purification of substances by a gas separation method', *Desalination*, vol. 240, no. 1–3, pp. 301–305, <a href="https://doi.org/10.1016/j.desal.2007.12.043">https://doi.org/10.1016/j.desal.2007.12.043</a> Vorotyntsev, VM, Drozdov, PN, Vorotyntsev, IV & Smirnov, KY 2006b, 'Germane high purification by membrane gas separation', *Desalination*, vol. 200, no. 1–3, pp. 232–233,

https://doi.org/10.1016/j.desal.2006.03.307

Yahaya, GO, Choi, SH, Ben Sultan, MM & Hayek, A 2020, 'Development of thin-film composite membranes from aromatic cardo-type co-polyimide for mixed and sour gas separations from natural gas', *Global Challenges*, vol. 4, no. 7, article 1900107, <a href="https://doi.org/10.1002/gch2.201900107">https://doi.org/10.1002/gch2.201900107</a>

Yamada, H, Higashii, T, Chowdhury, FA, Goto, K & Kazama, S 2012, 'Experimental study into carbon dioxide solubility and species distribution in aqueous alkanolamine solutions', *WIT Transactions on Ecology and the Environment*, vol. 157, pp. 515–523, <a href="https://doi.org/10.2495/air120451">https://doi.org/10.2495/air120451</a>

Zou, C, Xiong, B, Xue, H, Zheng, D, Ge, Z, Wang, Y, Jiang, L, Pan, S & Wu, S 2021, 'The role of new energy in carbon neutral', *Petroleum Exploration and Development*, vol. 48, no. 2, pp. 480–491, https://doi.org/10.1016/s1876-3804(21)60039-3